Pergamon

Int. J. Solids Structures Vol. 34, No. 8, pp. 931–947, 1997

0020–7683/97 $17.00 + .00

PII: S0020–7683(96)00066–2

A VISCOELASTIC CONSTITUTIVE MODEL FOR PARTICULATE COMPOSITES WITH GROWING DAMAGE

S. W. PARK
Department of Civil Engineering, North Carolina State University, Raleigh, NC 27695-7908, U.S.A.

and

R. A. SCHAPERY
Department of Aerospace Engineering and Engineering Mechanics, The University of Texas at Austin, Austin, TX 78712, U.S.A

(*Received* 21 *July* 1995; *in revised form* 24 *April* 1996)

Abstract—A mechanical model which describes time- and temperature-dependent deformation behavior of particulate composites with changing microstructure, including growing damage, is described and then verified by experimental study of a viscoelastic filled elastomer. An existing constitutive model, which is based upon thermodynamics of irreversible processes with internal state variables, is first reviewed and then used to describe the mechanical behavior of elastic and viscoelastic media with changing microstructure. A rate-type equation is successfully employed in describing the evolution of microstructural changes, which are believed here to be primarily microcracking. An elastic-viscoelastic correspondence principle and the time-temperature superposition principle are used in modeling effects of the material's intrinsic viscoelasticity and the effects of temperature changes. Laboratory tests of the stress and dilatation responses of uniaxial test specimens under controlled monotonically increasing axial extension and constant confining pressure at different temperatures were performed. The effects of strain level, strain rate, confining pressure, and temperature on the stress and dilatation are described and compared to the theoretical model.

1. INTRODUCTION

Particulate composites consist of particles of one or more materials suspended in a matrix of another material. The mechanical behavior of these composites depends upon their constituents' properties and any microstructural changes that may occur in the body under loading. When the composite is subjected to thermo-mechanical loading, the internal structure of the composite may change due to high stress concentrations that develop along the particle-matrix interfaces or within the matrix or particles. The mechanism of these changes depends upon the type of composite. Our emphasis here will be placed on composites, like solid propellant, made of a high volume fraction of strong, rigid particles randomly suspended in a rubber matrix. The mechanical behavior of such filled rubber has been studied extensively over many years. Vacuole formation and growth (Farris, 1968), the Mullins effect (Mullins, 1969), viscoelasticity (Schapery, 1974, 1982, 1990b), strain softening (Swanson and Christensen, 1983), thermal-mechanical interaction (Hufferd, 1980), and finite deformations (Peng, 1985, 1992, Simo, 1987) all contribute to the complex behavior of filled rubber. Damage in highly-filled rubber appears to be primarily in the form of microcracks initiating and growing within the matrix and along the particle-matrix interfaces (e.g., Cornwell and Schapery, 1975).

The cause of initiation and growing of microcracks in filled rubber under mechanical loading is relatively well established. When such a material is stretched, high triaxial stress concentrations develop in the binder near or at the surface of each filler particle. Cracks and voids in the elastic range of behavior are believed to initiate when this stress exceeds a critical value (which is approximately equal to rubber's Young's modulus as a result of a

local geometrical instability (Gent and Lindley, 1958, Schapery, 1991)). If hydrostatic pressure is applied while the material is deformed, the pressure will retard void formation.

Void formation is of interest because of its effects on overall deformation behavior. The behavior of filled rubber is complicated not only due to microcracking but also to the viscoelasticity of the rubber matrix. Furthermore, the mechanisms are coupled, and the deformation and failure behavior are dependent upon the history of loading. Also, when the composite is subjected to nonisothermal conditions, the constitutive equations must be modified to duly account for temperature effects on the material properties; normally temperature affects the intrinsic time-scale of viscoelastic materials. In order to deal with such a complication, we need to use a constitutive model which has a sound physical basis and an amenable theoretical framework so that the model can be characterized by experimental data without excessive difficulty.

Schapery (1987a, 1990a) developed a constitutive theory for elastic media with growing damage and other changes in structure, and then extended it to a class of viscoelastic media. His theory for elastic media is based on thermodynamics of irreversible processes with an internal state variable description of the structural changes, and was motivated from the observation that, for limited load histories, the total work input to a composite body which undergoes structural changes is insensitive to the input load history. The theory was used in describing the behavior of particulate- and fiber-reinforced composites with growing damage (Schapery, 1987a, 1987b, 1989). The theory is general enough to allow for strong nonlinearities and coupling between the internal state variables and for it to describe a variety of mechanisms including micro- and macro-crack growth in monolithic and composite materials. Schapery and Sicking (1995) applied the theory to model material nonlinearity in graphite-epoxy laminates, and Lamborn and Schapery (1988, 1993) showed the existence of a work potential for suitability limited deformation paths using experimental data from axial and torsional deformation tests on angle-ply fiber-reinforced plastic laminates.

This elastic model with damage growth and other microstructural changes has been generalized to account for thermo-viscoelastic characteristics (Schapery, 1990a,b). Here we propose and apply an explicit representation of this generalized model to the characterization of a crosslinked, amorphous rubber filled with seventy percent volume fraction of hard particles.

A series of mechanical tests was performed in order to determine all the material-dependent functions and constants that appear in the model. The specimens were subjected to axial straining under a fixed hydrostatic pressure. Different combinations of constant strain rates, pressures and temperatures were applied. Characterization of the material using these experimental data is described. Then the mechanical response is predicted for strain histories and temperatures not used in the characterization process and compared to experimental results.

2. A CONSTITUTIVE MODEL FOR MATERIALS WITH CHANGING MICROSTRUCTURE

2.1. *The work potential model*

Following Schapery (1990a), the mechanical behavior is first expressed in terms of relationships between generalized forces Q_j ($j = 1, 2, \ldots, J$) and generalized displacements q_j ($j = 1, 2, \ldots, J$). This formulation is then adapted in Section 2.2 to the specific geometry and loading conditions studied experimentally. For all processes of interest, the existence of a strain energy density function W is assumed, with the property that

$$Q_j = \frac{\partial W}{\partial q_j} \tag{1}$$

where W is a state function of independent generalized displacements q_j and internal state variables (ISVs) S_m ($m = 1, 2, \ldots, M$). The ISVs serve to account for the effects of damage and other microstructural changes.

For an arbitrary infinitesimal process with changes in q_j and S_m,

$$dW = \frac{\partial W}{\partial q_j} dq_j + \frac{\partial W}{\partial S_m} dS_m = Q_j dq_j - f_m dS_m \tag{2}$$

where $f_m \equiv -\partial W/\partial S_m$ is so-called *thermodynamic* force. We specify as the damage (or internal state) evolution law

$$f_m = \frac{\partial W_S}{\partial S_m} \quad \text{when } \dot{S}_m \neq 0 \tag{3}$$

where W_S is a state function of S_m. The left side of (3) is the available force for producing changes in S_m while the right hand side is the required force (as in the case of a crack growth equation).

The total work done on the body by Q_j during an actual process (i.e., a process for which S_m changes according to (3)), starting at some reference state, is

$$W_T \equiv \int Q_j dq_j. \tag{4}$$

From (2)–(4), we find that W_T is a function of the state (q_j, S_m), and is given by

$$W_T = W + W_S \tag{5}$$

where $W = W_S = 0$ in the reference state. Thus, W_S may be interpreted as that portion of the total work which contributes to changes in the structure. It is observed that (3) represents equations for finding S_m as functions of q_j; thus, $W_T = W(q_j, S_m(q_j)) + W_S(S_m(q_j))$ or simply $W_T = W_T(q_j)$. The total work W_T is not only a state function of q_j and S_m but it is a potential in q_j during inelastic processes. Then from (4)

$$Q_j = \frac{\partial W_T}{\partial q_j} \tag{6}$$

showing that the body exhibits hyperelastic behavior during the time any particular set of parameters S_m undergoes change. Because the total work is a potential in q_j, the incremental stiffness matrix is symmetric. Conversely, given that this stiffness matrix is symmetric when one or more S_m change, then both (3) and (6) follow. Either (1) or (6) may be used in characterizing or predicting mechanical behavior of an elastic body with changing structure.

According to the second law of thermodynamics, only those changes in S_m that correspond to a non-negative entropy production rate are possible, i.e.,

$$TS_{ent} = f_m \dot{S}_m \geqslant 0 \tag{7}$$

where, T is absolute temperature, S_{ent} is the entropy production rate, and the overdot denotes a time derivative. From (3) and (7), it is seen that the energy dissipation W_S never decreases in any physical process.

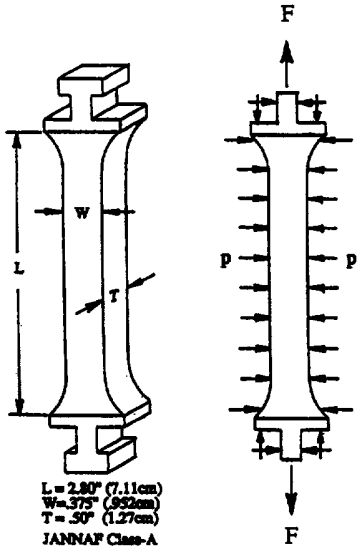

Fig. 1. Specimen geometry and loading.

2.2. *An elastic bar under axial extension and pressure*

A theoretical model for the mechanical behavior of an elastic bar with growing damage under axial extension and an all-around pressure, as shown in Fig. 1, was developed by Schapery (1987b) using his work potential theory. Here the elements of the model are presented as they will serve as the basis for our subsequent extension to the corresponding viscoelastic damage model.

Consider a uniaxial specimen which is subjected to specified axial displacement ΔL and all-around pressure p. As generalized displacements, select the *nominal* strain ε, and dilatation v, defined by

$$q_1 = \varepsilon \equiv \frac{\Delta L}{L_0}, \quad q_2 = v \equiv \frac{\Delta V}{V_0} \tag{8}$$

where ΔL and ΔV are the increase in specimen length and volume from the initial undeformed state in which the gage length is L_0 and volume is V_0. The corresponding generalized forces are

$$Q_1 = \sigma \equiv \frac{F}{A_0}, \quad Q_2 = -p \tag{9}$$

where A_0 is the initial cross-sectional area of the specimen, σ is the *nominal* stress, and F is the axial force above that due to the pressure ($F = 0$ when the only loading is due to p). Equations (8) and (9) are not limited to small strains as their choices satisfy the work conjugate requirement regardless of strain level.

The strain energy density is taken as a function of ε, v, and S, i.e., $W = W(\varepsilon, v, S)$ according to the previous discussion. In this example, one ISV, S, is assumed to be sufficient to characterize the microstructural state of the specimen subjected to the specified loading. The loading induces axisymmetric damage on the average, and the initially isotropic material becomes transversely isotropic. For this case of one ISV, we may take $S = W_S$ without loss of generality. Recall that W_S is the dissipated work due to damage or other change in the microstructure. Then from (3)

$$-\frac{\partial W}{\partial S} = 1 \quad \text{when } \dot{S} \neq 0 \tag{10}$$

and the stress-strain relations are obtained from (1), (8) and (9),

$$\sigma = \frac{\partial W}{\partial \varepsilon}, \quad p = -\frac{\partial W}{\partial v}. \tag{11}$$

Since ε and p are controlled variables in this example, it is helpful to rewrite the theory so that they appear as the independent variables. We thus introduce a *dual energy* density function $W_D = W_D(\varepsilon, p, S)$, defined by

$$W_D \equiv W + pv. \tag{12}$$

From the relationships in (11) and the total differential of (12), one obtains

$$\sigma = \frac{\partial W_D}{\partial \varepsilon}, \quad v = \frac{\partial W_D}{\partial p}, \quad \frac{\partial W}{\partial S} = \frac{\partial W_D}{\partial S}. \tag{13}$$

From (10) and (13)

$$-\frac{\partial W_D}{\partial S} = 1 \quad \text{when } \dot{S} \neq 0. \tag{14}$$

The total dual work is defined by

$$W_{TD} \equiv W_T + pv \tag{15}$$

so that from (4)

$$W_{TD} = \int \sigma d\varepsilon + \int v dp \tag{16}$$

and then using (5) and $W_S = S$

$$W_{TD} = W_D + S. \tag{17}$$

As the dual energy function W_D, the following form was adopted by Schapery (1987b),

$$W_D = C_{11}(S) \int_0^{\varepsilon} g(\varepsilon')\varepsilon' d\varepsilon' + C_{12}(S)\varepsilon p + \frac{1}{2} C_{22}(S) p^2 \tag{18}$$

where the coefficients C_{ij} $(i,j = 1,2)$ are functions of S and g a function of ε. From (13)

$$\sigma = C_{11}(S)g(\varepsilon)\varepsilon + C_{12}(S)p \tag{19}$$

$$v = C_{12}(S)\varepsilon + C_{22}(S)p \tag{20}$$

which, for fixed S and $g = 1$, are equations for a transversely isotropic, linear elastic material. As will be shown later for viscoelastic behavior, the strain-dependent material function $g(\varepsilon)$ must be replaced by a function of a second ISV; these functions for elastic and viscoelastic behavior decrease with straining, and serve to characterizing the nonlinear behavior at high pressures.

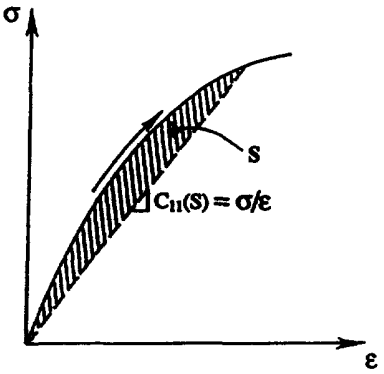

Fig. 2. A stress-strain curve for uniaxial loading. The dashed line is not necessarily the unloading curve. (The variable S is equal to the total work of microstructural changes.)

Equations (19) and (20), together with (14) and (18), were used by Schapery (1987b) with experimental data for solid propellant in the elastic range of behavior to obtain the material functions, $g(\varepsilon)$, $C_{11}(S)$, $C_{12}(S)$, and $C_{22}(S)$ and thus to completely define W_D. Figure 2 illustrates the relationship between W_{TD}, W_D, and S for $g = 1$ and $p = 0$; the instantaneous value of S is equal to the shaded area, $W_{TD} - W_D$. Once the dual energy function W_D is determined, one can predict stress and dilatation responses for the given strain and pressure using (19) and (20) and the S-evolution law, (14).

2.3. *A viscoelastic bar under axial extension and pressure at different temperatures*

Our objective here is to establish an extended model which adequately accounts for the effects of viscoelasticity and temperature. The presence of viscoelasticity influences the form of the strain energy function and the ISV evolution law. The intrinsic time-scale of viscoelastic materials, in general, changes dramatically with temperature. Schapery (1981, 1990b) developed some guidelines for generalizing an elastic model to accommodate viscoelasticity, temperature effects, and microcrack growth through the use of micromechanics, an elastic-viscoelastic correspondence principle, thermal expansion, the time-temperature superposition (i.e., so-called *thermorheological simplicity*), and rate-dependent ISV evolution laws. Thermal expansion is neglected in the present formulation for simplicity.

Based on these guidelines, first we shall replace the strain in the elastic formulation with pseudo-strain defined by the following:

$$\varepsilon^R = \frac{1}{E_R}\int_0^t E(\xi - \xi')\frac{d\varepsilon}{d\tau}d\tau \tag{21}$$

where

$$\xi(t) \equiv \int_0^t \frac{dt'}{a_T(T)} \tag{22}$$

and $\xi' \equiv \xi(\tau)$. Also, $E(\xi)$ is the relaxation modulus and E_R is the *reference modulus* which is a free constant and has the same dimension as the relaxation modulus. The quantities t, ξ, and a_T are physical time, reduced time, and the time-temperature shift factor, respectively; the a_T reflects the influence of temperature on internal viscosity of the rubber. A pseudo-dilatation is defined in the same manner as the pseudo-strain except the strain is replaced by dilatation. Then, according to an appropriate elastic-viscoelastic correspondence principle, with or without microcrack growth (Schapery, 1984), the equations for an elastic composite can be used for the corresponding viscoelastic composite in terms of pseudo-strain and dilatation.

The ISV evolution for elastic materials, however, cannot directly be translated into an evolution law for viscoelastic materials by the procedure described above without further

modification. It is to be understood that not only is the available force for growth in S rate-dependent, but the resistance against the growth of S is rate- or time-dependent. The equation which is used in the following work is like the well-known power-law crack growth equation for viscoelastic materials (e.g., Schapery 1975, 1984), specifically,

$$\dot{S} = \left(-\frac{\partial W_D}{\partial S} \right)^{\alpha} \tag{23}$$

where W_D is the dual energy density function, the overdot denotes a reduced time derivative and α is a constant. It has been shown by Schapery (1990b) that when α is much greater than unity, (23) may be replaced by (14), but with a time-dependent right-hand side. Inclusion of an S-dependent factor on the right side of (23) does not really generalize (23) because one may always eliminate it through a change of the ISV.

The following equations constitute the viscoelastic model used in the characterization of the filled elastomer under study.

Pseudo dual energy function:

$$W_{RD}(\varepsilon^R, p, S_1, S_2) = C_{11}(S_1)C(S_2)\frac{(\varepsilon^R)^2}{2} + C_{12}(S_1)\varepsilon^R p + C_{22}(S_1)\frac{p^2}{2}. \tag{24}$$

Stress-strain relations:

$$\sigma = \frac{\partial W_{RD}}{\partial \varepsilon^R} = C_{11}(S_1)C(S_2)\varepsilon^R + C_{12}(S_1)p \tag{25}$$

$$v^R = \frac{\partial W_{RD}}{\partial p} = C_{12}(S_1)\varepsilon^R + C_{22}(S_1)p. \tag{26}$$

ISV evolution laws:

$$\dot{S}_1 = \left(-\frac{\partial W_{RD}}{\partial S_1} \right)^{\alpha_1} \quad \text{when } \dot{S}_1 \neq 0 \tag{27}$$

$$\dot{S}_2 = \left(-\frac{\partial W_{RD}}{\partial S_2} \right)^{\alpha_2} \quad \text{when } \dot{S}_2 \neq 0. \tag{28}$$

It is seen that (25) and (26) are like (19) and (20) for elastic behavior, but pseudo variables replace physical strain and dilatation, and there are two, rather than one, ISVs or damage parameters. Additionally, the second parameter S_2 appears as the argument of only the factor C. This factor replaces $g(\varepsilon)$ used in the original elastic formulation, and thus the equations are like *linear* elastic equations when the damage is constant. As before (Schapery, 1991) we find that the coefficients C_{ij} found from the experimental data are similar to those predicted from a simple micromechanical model for which all nonlinearity is due to microcrack-like voids, and their argument is a measure of the work of forming the void surfaces. If the pressure is high enough, these voids do not form with axial straining, implying that $S_1 \equiv 0$. Without damage-induced voids, the bulk modulus of the composite is high enough to neglect the dilatation relative to that due to voids. Thus, for our purposes we may assume $C_{12}(0) = C_{22}(0) = 0$. Under such high pressures all nonlinearity in the earlier elastic characterization was expressed in terms of $g(\varepsilon)$. However, our experimental data show that this nonlinearity is strain rate-dependent in a manner that cannot be accounted for using only pseudo-strain. Thus, $C(S_2)$ is introduced, along with a rate-like evolution law (28); this characterization of the high-pressure behavior is shown later to be consistent with the data. The observed softening behavior that is accounted for using $C(S_2)$

possibly represents shearing micromechanisms such as shear cracking, chain breakage and disentanglement, as well as slipping along particle-rubber interfaces.

3. MODEL CHARACTERIZATION AND PREDICTION

3.1. *Material and laboratory experiments*

The material used in the research was provided by the Naval Weapons Center. It is an inert solid propellant with 70 volume percent of particles of aluminium, potassium sulfate, and ammonium sulfate, embedded in a lightly-crosslinked HTPB (Hydroxy-Terminated Poly-Butadiene) binder. The size of particles ranges from 20 microns to 200 microns. Having a volume fraction of 70%, significant local stress concentrations develop especially along the particle-matrix interfaces and the movement of rubber is well constrained. Although there is good bonding between particles and the rubber matrix, the high degree of packing and its accompanying stress concentrations result in the development of distributed microcrack-like void growth at strains well below those which cause global specimen rupture (Cornwell and Schapery, 1975).

The material possesses a significant amount of viscoelasticity due to the presence of the rubber matrix. The relaxation modulus $E(\xi)$ and the time-temperature shift factor $a_T(T)$ were measured using a dynamic mechanical analyzer manufactured by Rheometrics Inc. These measurements were based upon a small-amplitude sinusoidal strain input history and the principles of the *linear* viscoelasticity theory. A temperature(T)-frequency(ω) sweep dynamic test provided data required to generate the *master* complex modulus $E^*(\lambda)$ and the shift factor $a_T(T)$, where $\lambda = \omega a_T$. The frequency-dependent master complex modulus $E^*(\lambda)$ was then converted to the time-dependent master relaxation modulus $E(\xi)$ through their inter-relationship based on the theory of linear viscoelasticity (e.g., Ferry, 1980). The reduced time is $\xi = t/a_T$ because the temperature is constant. Figures 3 and 4 present $E(\xi)$ and $a_T(T)$, respectively. The detailed procedure for obtaining $E(\xi)$ and $a_T(T)$ for the material used in this research is given by Park (1994).

The stress-strain-dilatation behavior of the propellant under different loading and temperature conditions was measured using a Farris gas dilatometer attached to an Instron, screw-type tester. Specimens of JANNAF (Joint Army-Navy-NASA-Air Force Propulsion Committee) Class-A type were subjected to axial stretching and hydrostatic pressure at different temperatures. The geometry of a specimen and loading condition are schematically shown in Fig. 1. Two types of tensile tests, a constant strain rate history and a dual strain rate history, were performed. Part of the constant strain rate test results was used in the characterization of the theoretical model. The remaining test results were used to verify the

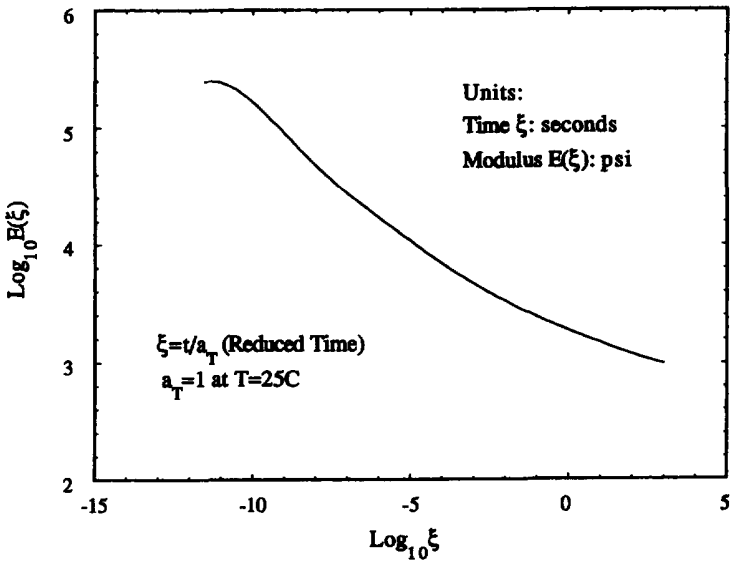

Fig. 3. Master relaxation function, $E(\xi)$.

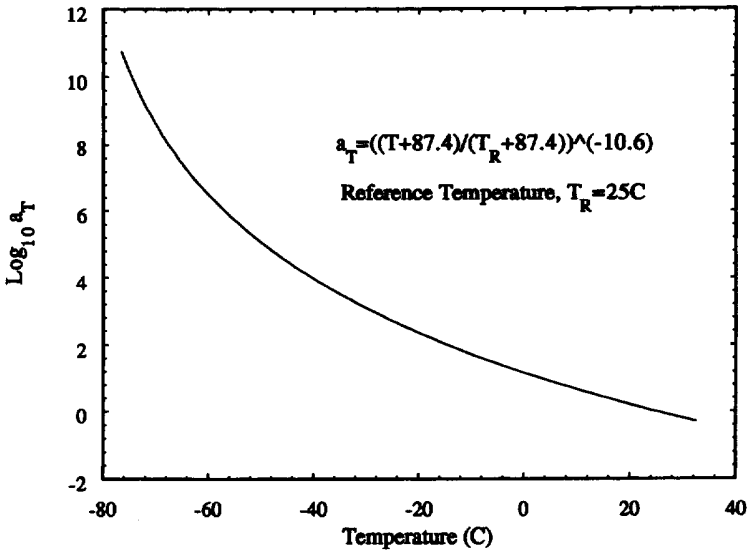

Fig. 4. Time-temperature shift factor, a_T.

model. Various combinations of different test parameters were applied. The test parameters include strain rate, confining pressure, and temperature. Four different strain rates (0.0006/sec, 0.006/sec, 0.06/sec, and 0.24/sec corresponding to the crosshead rates of 0.1″/min, 1″/min, 10″/min, and 40″/min, respectively), four different pressures (0 psi, 75 psi, 200 psi, and 800 psi in gage pressure), and four different temperatures (25°C, −10°C, −25°C, and −40°C) were employed. The test results are presented and discussed together with their corresponding theoretical predictions in a later section.

3.2. *Determination of material functions and constants*

In view of the proposed model, as represented by (24)–(28) there are a total of six quantities to be determined. They are four functions, $C_{11}(S_1)$, $C_{12}(S_1)$, $C_{22}(S_1)$, $C(S_2)$, and two constants, α_1 and α_2. These quantities are all dependent upon the specific material that is used, and should be found using the data obtained from experiments performed on that material. A simultaneous determination of all the quantities is not practical. Instead, a step-by-step sequential characterization can be performed using some simplifying features and conditions.

The material functions $C_{ij}(S_1)$ $(i,j = 1,2)$ and $C(S_2)$ can be found by using a set of experimental data on stress and dilatation responses and the postulated evolution laws on S_1 and S_2. Equations (25) and (26) together with the experimental data on stress and dilatation give C_{ij} and C with dependence on ε and p. In order to find their dependence on S_1 and S_2, we need to first obtain the values of S_1 and S_2 corresponding to ε and p input by solving the evolution laws. However, the rate-type evolution laws (27) and (28) are not convenient for finding S_1 and S_2 that are needed in the process of characterization because the equations themselves require an *a priori* knowledge of $C_{ij}(S_1)$ and $C(S_2)$ before the equations can be solved for S_1 and S_2. The characterization appears to require an exhaustive iteration process, which would be highly inefficient and impractical. However, using an approximation developed by Schapery (1990b), it can be shown that the rate-type evolution laws (27) and (28) can be converted to the following integrated forms, which are similar to (14) for elastic behavior,

$$-\frac{\partial W_{RD}}{\partial \hat{S}_1} = \xi^{-1/\alpha_1} \quad \text{when } \dot{S}_1 \neq 0 \tag{29}$$

$$-\frac{\partial W_{RD}}{\partial \hat{S}_2} = \xi^{-1/\alpha_2} \quad \text{when } \dot{S}_2 \neq 0 \tag{30}$$

where

Table 1. Analytical representations of the material functions

$C_{11}(S_1) = 2100 - 803\, S_1^{1/5} + 1578\, S_1^{2/5} - 1910\, S_1^{3/5} + 545\, S_1^{4/5}$
$C_{12}(S_1) = 0.0744\, S_1^{1/2} + 0.0333\, S_1 - 0.00248\, S_1^{3/2}$
$C_{22}(S_1) = -1.705\text{E-}5\, S_1^{1/2} - 1.544\text{E-}5\, S_1 - 1.109\text{E-}6\, S_1^{3/2}$
$C(S_2) = 1 + 0.0937\, S_2^{2/5} - 0.385\, S_2^{2/5} + 0.0776\, S_2^{3/5}$

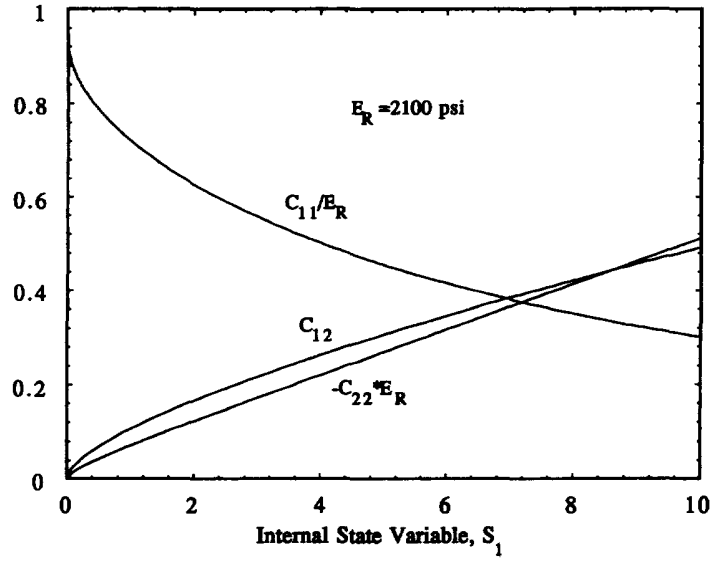

Fig. 5. Material functions, $C_{11}(S_1)$, $C_{12}(S_1)$, and $C_{22}(S_1)$.

$$\hat{S}_1 \equiv \frac{1}{1+\frac{1}{\alpha_1}} S_1^{(1+(1/\alpha_1))} \quad \text{and} \quad \hat{S}_2 \equiv \frac{1}{1+\frac{1}{\alpha_2}} S_2^{(1+(1/\alpha_2))}. \tag{31}$$

In deriving (29) and (30) from (27) and (28), it was assumed that $(\alpha_1, \alpha_2) \gg 1$. Therefore, the evolution laws (29) and (30) should be viewed as an *approximate* version of (27) and (28), respectively. If the evolution laws (29) and (30) are used, the characterization process will be much simpler and straightforward. Indeed, we can first find the four functions and constants using the evolution laws (29) and (30) and then refine them using the original rate-type evolution laws (27) and (28). The detailed procedure for determination of the material functions and constants is given by Park (1994). The values of α_1 and α_2 were determined to be 6 and 4.5, respectively, and the functions $C_{ij}(S_1)$ and $C(S_2)$ are given in Table 1 and graphically represented in Figs 5 and 6 over the range of S_1 and S_2 found from the experimental data. Third- or fourth-order polynomial expansions in different fractional powers of S_1 and S_2 were used to obtain an analytical representation of each function. These C_{ij} are similar to those predicted from a simple micromechanical model where S_1 is a measure of the work of microcracking (Schapery, 1991). It should be added that $C_{11} = E_R$ (where E_R is the initial slope in the stress-pseudo strain curve), $C_{12} = C_{22} = 0$ for the highest pressure ($p = 800$ psi), and therefore, $C(S_2)$ can be obtained from the experimental stress-strain curve together with (25), in which case $\sigma = E_R\, C(S_2)\, \varepsilon^R$. Also, according to (27) and (28), the units for both S_1 and S_2 are of [Stress]$^{\alpha/(\alpha+1)}$ [Time]$^{1/(\alpha+1)}$. The units for C_{11} are the same as those of stress, and the units for C_{22} are the reciprocal of those for C_{11}. Functions C_{12} and C are dimensionless.

3.3. *Prediction of mechanical responses and damage evolution*

Once all the necessary material-dependent functions and constants that appear in the theoretical model are determined we may predict stress and dilatation responses to different input histories. The overall prediction steps are as follows:

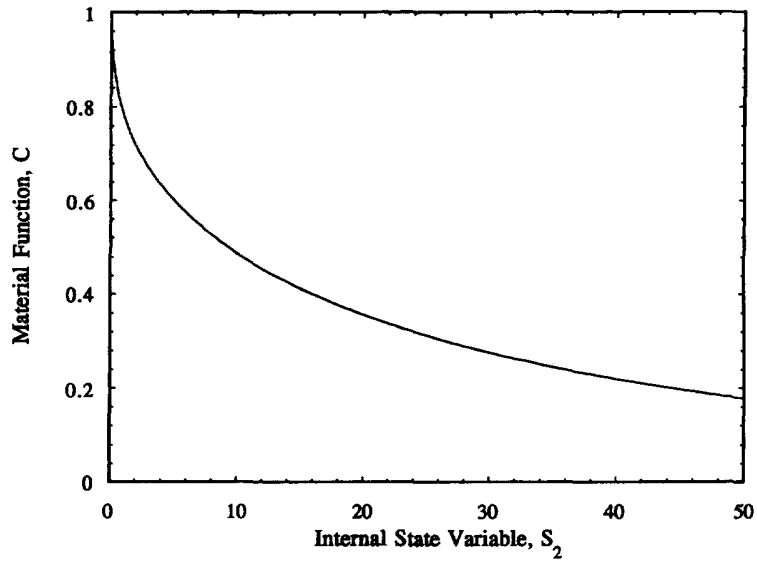

Fig. 6. Material function, $C(S_2)$.

1. For a given input strain history, compute pseudo strain ε^R according to (21).

2. For given (ε^R, p), obtain S_1 and S_2 using (27) and (28). Summation of incremental values of S_1 and S_2, over the time elapsed since the load has been imposed is to be carried out with initial conditions of $S_1|_{t=0} = S_2|_{t=0} = 0$.

3. Substitute $(S_1, S_2, \varepsilon^R, p)$ into (25) and (26), and obtain instantaneous values of σ and v^R.

4. The physical dilatation v may be obtained from v^R according to the inverse form of (21) with ε replaced by v, i.e.,

$$v = E_R \int_0^t D(\xi - \xi') \frac{\mathrm{d}v^R}{\mathrm{d}\tau} \mathrm{d}\tau. \tag{32}$$

Equation (32) may be replaced by an appropriate numerical integration scheme. The function $D(\xi)$ may be obtained from $E(\xi)$ using their inter-relationship,

$$\int_0^\xi E(\xi - \xi') \mathrm{d}D(\xi')/\mathrm{d}\xi' \mathrm{d}\xi' = H(\xi) \tag{33}$$

where $H(\xi)$ is the Heaviside step function.

Some sample predictions of stress and dilatation responses to constant-rate axial extension and hydrostatic pressure at room temperature are presented together with their corresponding experimental data in Figs 7–10. In each plot, the discrete symbols represent experimental data, typically an average from five different specimens, and the continuous lines give the theoretical predictions. The same graphic scales were maintained for a convenient comparison. Overall, the predictions are considered to be very good taking into account the intrinsic variability in the mechanical behavior of solid propellant. The stress for $p = 0$ and the dilatation for $p = 0$ and $p = 75$ psi in Fig. 7 were used in determining the three material functions $C_{ij}(S_1)$; the stress for $p = 800$ psi was used to find $C(S_2)$. The small discrepancy between the theory and experiment for these cases is due to the smoothing effects associated with curve-fitting in the characterization process. Some sample predictions of the structural parameters S_1 and S_2, which are obtained from the evolution laws (27) and (28), are given in Figs 11 and 12. It is seen that the variation of S_1 is similar to that of dilatation, as anticipated from a micromechanical model (Schapery, 1991). The parameter S_1 decreases with pressure but S_2 slightly increases with pressure, for given strain and strain rate. Also, it was seen (Park, 1994) that S_1 increases with strain rate but S_2 slightly decreases

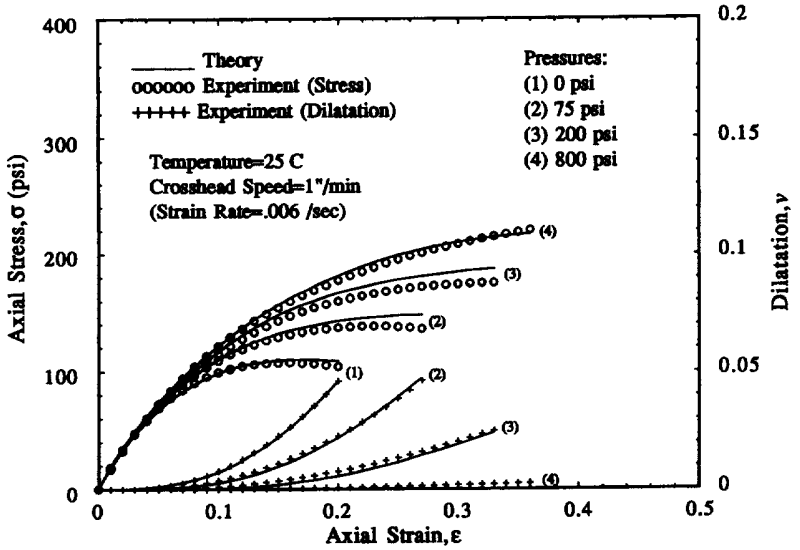

Fig. 7. Stress-strain-dilatation behavior under axial extension and hydrostatic pressure (at $d\varepsilon/dt = 0.006$/sec and $T = 25°C$).

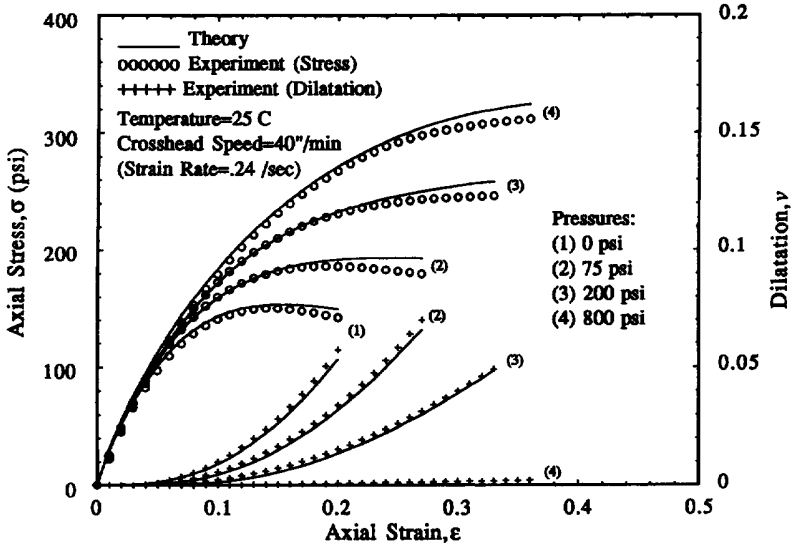

Fig. 8. Stress-strain-dilatation behavior under axial extension and hydrostatic pressure (at $d\varepsilon/dt = 0.24$/sec and $T = 25°C$).

with strain rate, for given strain and pressure. Therefore, it is believed that at high pressures the dilatation-type material damage is relatively insignificant, but non-dilatational microstructural changes including shear damage and polymer chain disentanglements may be appreciable.

A study of the material's mechanical behavior at low temperatures is of considerable interest for low temperature storage and firing of rocket motors. Also, it provides useful information in the propellant's behavior at very short time through a time-temperature superposition relationship. In describing the nonisothermal mechanical behavior of our material undergoing microstructural changes, we assume that the time-temperature superposition principle is still applicable. This assumption enables one to predict the mechanical behavior at different temperatures using the model characterized at one particular temperature as long as information on the shift factor a_T is available. It appears that the time-temperature superposition defined for the thermorheologically simple materials is also applicable to our material that undergoes significant microstructural changes, judging from the quality of predictions. The theoretical and experimental stress and dilatation responses

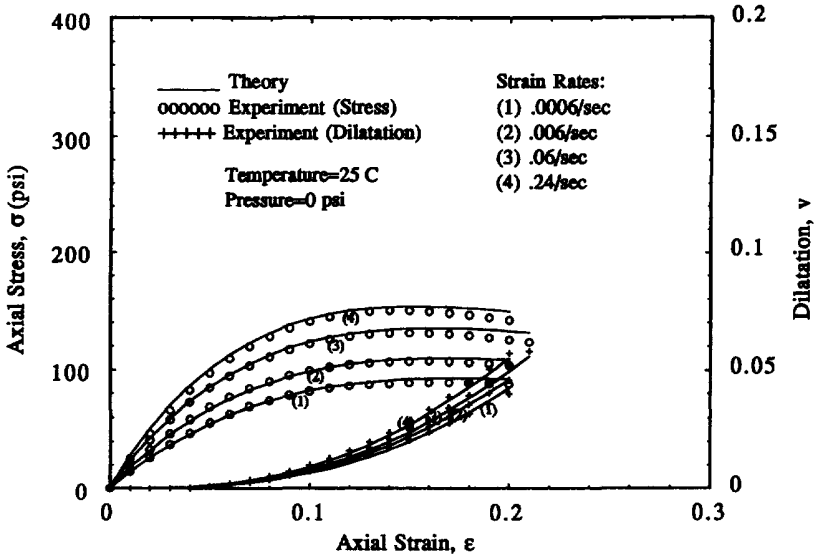

Fig. 9. Stress-strain-dilatation behavior under axial extension and atmospheric pressure (at $p = 0$ psi and $T = 25°C$).

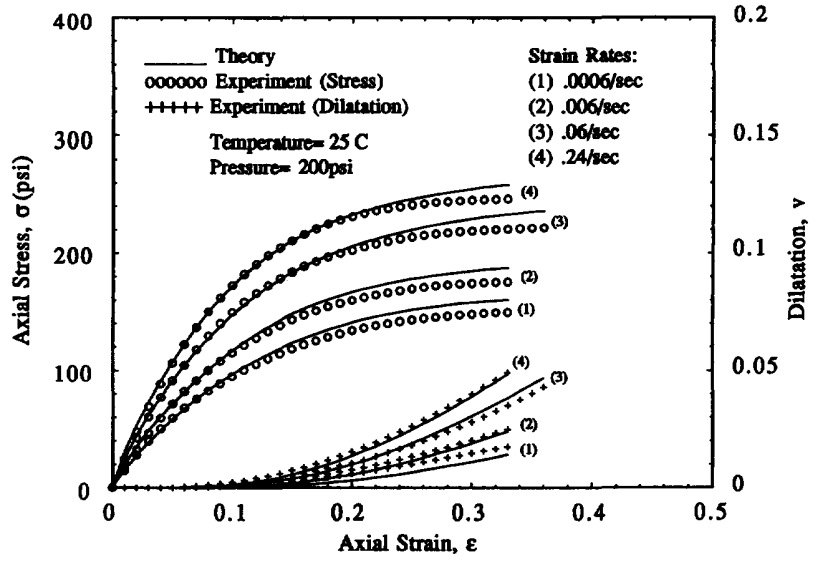

Fig. 10. Stress-strain-dilatation behavior under axial extension and hydrostatic pressure (at $p = 200$ psi and $T = 25°C$).

to constant-rate axial extension at four different temperatures, including room temperature, are presented in Figs 13 and 14. The overall quality of prediction is a little inferior to that of room temperature predictions. However, considering the fact that the a_T is from the linearly viscoelastic range of behavior (cf. Figs 3 and 4), the agreement is remarkably good, and certainly acceptable for use in engineering analysis.

We have characterized our model using a set of constant strain rate experimental data, and observed good agreement between theory and experiment for constant strain rate tests both at room and low temperatures not used in the nonlinear characterization. The growth of S_1 and S_2 is monotonic and smooth just as the stress and dilatation responses.

Now we shall test the model for its capability to describe the mechanical response to different types of strain input history other than those which were used in the characterization. Here we shall consider two different types of dual-rate strain input histories, as defined in Fig. 15, for atmospheric pressure and room temperature. The ratio of the two strain rates that constitute the input histories is 40, which is considered sufficiently large to

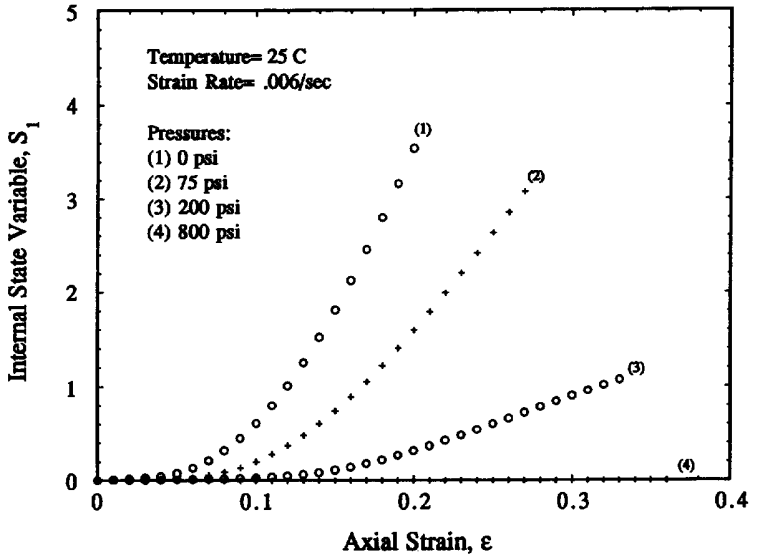

Fig. 11. Variation of S_1 with strain and pressure (at $d\varepsilon/dt = 0.006$/sec and $T = 25°C$).

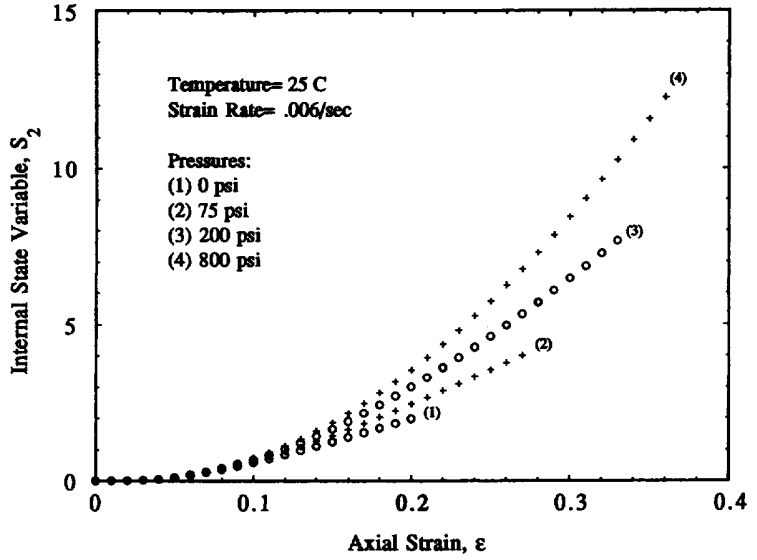

Fig. 12. Variation of S_2 with strain and pressure (at $d\varepsilon/dt = 0.006$/sec and $T = 25°C$).

induce responses distinctive from constant strain rate responses. Figures 16 and 17 present the experimental and theoretical stress-strain-dilatation responses to the two dual-rate strain input histories. The broken lines give the extensions of the theoretical predictions of the first part of the dual ramp straining, assuming the second part of the straining is at the same rate as the first part. The model is seen to be able to depict the sudden stress rise or drop at the point where the strain rate changes. It was observed that when the evolution laws (29) and (30) were used instead of (27) and (28) the predicted stress curve did not have enough sudden increase and decrease to match the experiments; this indicates that the rate-type evolution law should be adopted, at least in predicting responses to complex input histories. Of particular interest is the dilatation response beyond the discontinuity in strain rate. The experiments show that dilatation does not dramatically change its course beyond this point in both cases, and the theory is correct, in that it does not predict the type of abrupt changes which are observed in the stress curves. There is a sufficient change in slope to identify the dilatation curves when the strain rate changed. It is to be noted that the overall configuration of the response curves will be much dependent upon where the strain rate changes along the strain axis. For instance, if this point is at a very small strain

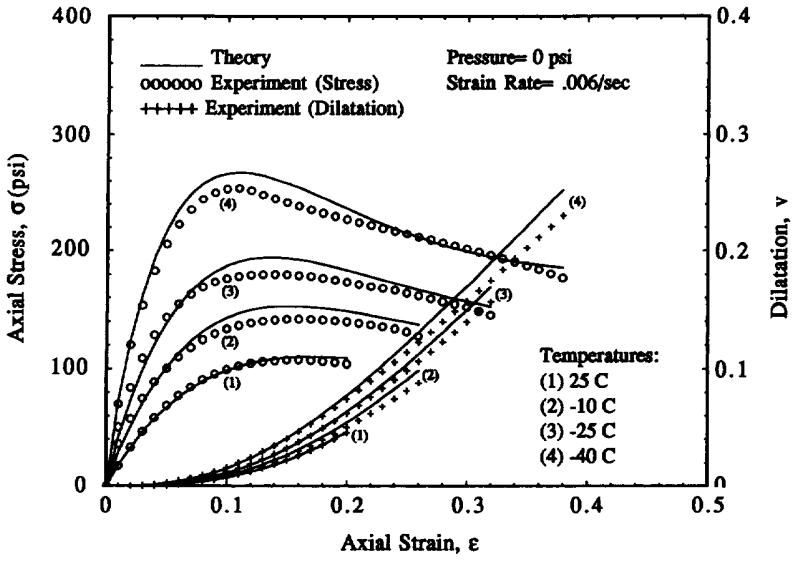

Fig. 13. Stress-strain-dilatation behavior under axial extension and atmospheric pressure at low temperatures (at $d\varepsilon/dt = 0.006$/sec and $p = 0$ psi).

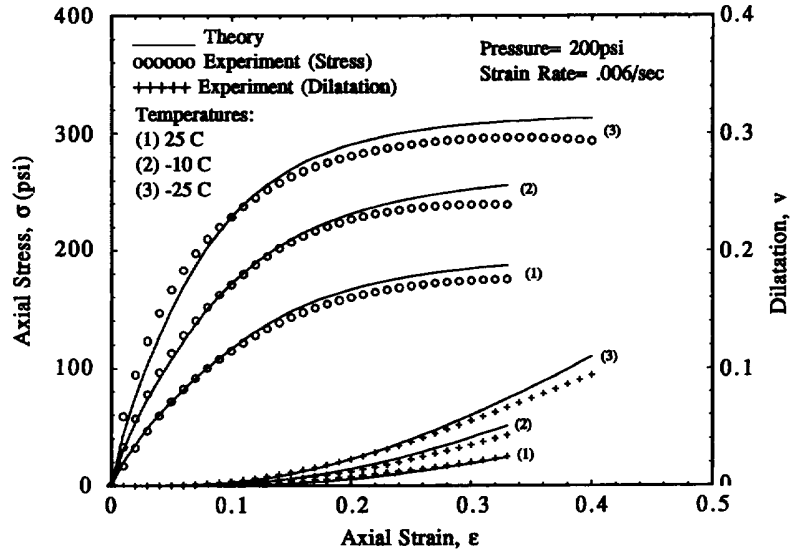

Fig. 14. Stress-strain-dilatation behavior under axial extension and hydrostatic pressure at low temperatures (at $d\varepsilon/dt = 0.006$/sec and $p = 200$ psi).

level or at a very large strain level, the effects of S_1 and S_2 on the resulting response may not be significant because the material may not have experienced any damage or it may have already experienced most of its damage. However, the intrinsic viscoelastic behavior may cause significant changes in the stress-strain-dilatation curves. Additional related experimental data and theoretical predictions are given by Park (1994).

4. CONCLUSIONS

A mathematical model that is based on thermodynamics with internal state variables and on viscoelastic micromechanics is shown to successfully describe the thermoviscoelastic behavior of a filled elastomer undergoing microstructural changes under axial stretching and pressure. The model is general in that it is potentially applicable to elastic and viscoelastic composites

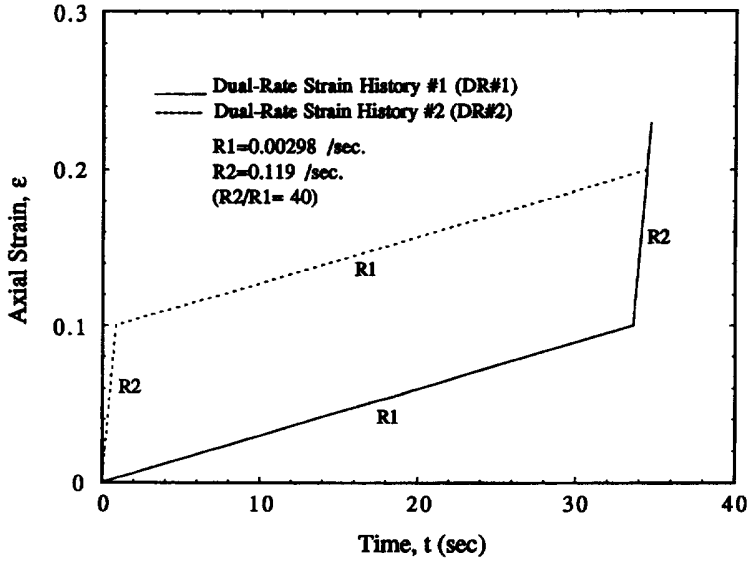

Fig. 15. Definitions of two dual-rate strain input histories.

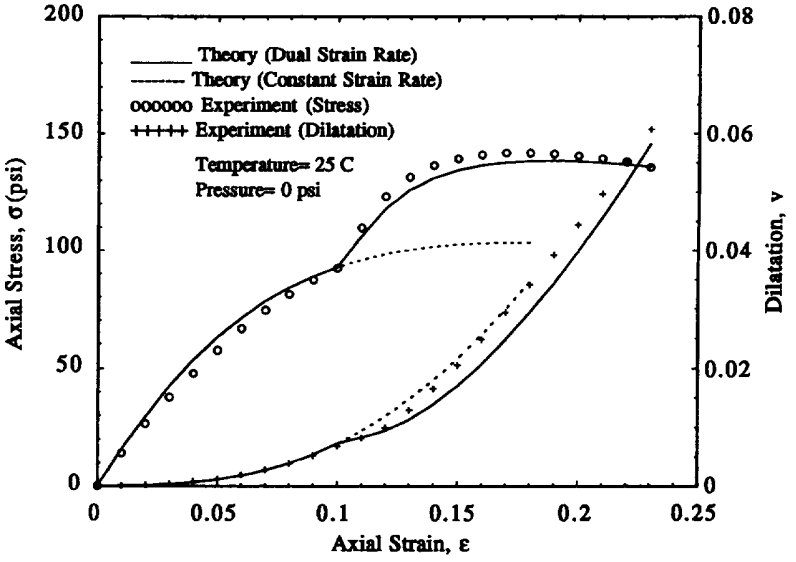

Fig. 16. Stress-strain-dilatation behavior under dual-rate axial extension [DR#1] (at $p = 0$ psi and $T = 25°C$).

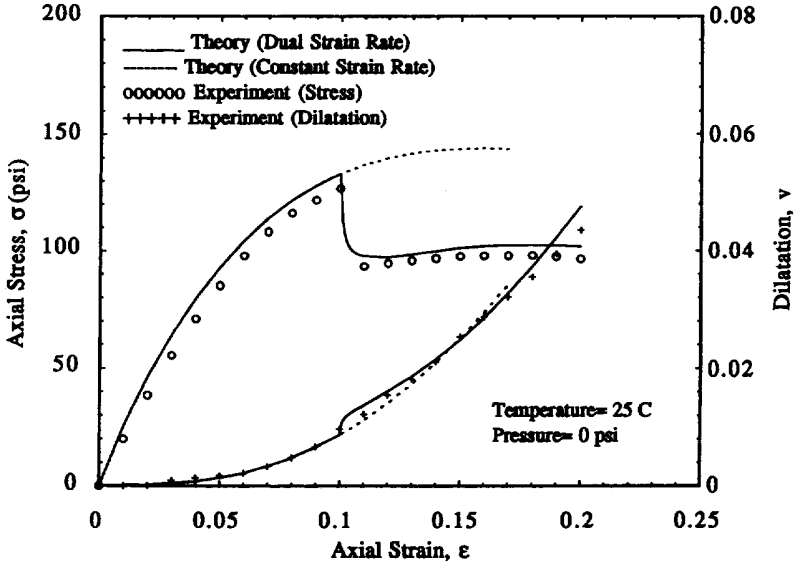

Fig. 17. Stress-strain-dilatation behavior under dual-rate axial extension [DR#2] (at $p = 0$ psi and $T = 25°C$).

with growing damage and other changes in structure at varying temperature. An elastic-viscoelastic correspondence principle (which led to the use of pseudo-strains) and the time-temperature superposition using a reduced-time have been found to be valid for describing the mechanical behavior of the material with damage. It has been demonstrated that a rate-type, power-law evolution law for the structural (or damage) parameters can be used successfully to predict the state of the material. Only constant strain rate and dual strain rate axial extensions with different pressures and temperatures were considered. Further study is required to extend the model to cover loading and unloading as well as general multiaxial loading. Approaches to making these extensions, in the context of a formulation that is similar to what is used here, have been discussed and used by Schapery (1982, 1987b, 1991).

Acknowledgements—This research was sponsored in part by the Office of Naval Research, Solid Mechanics Program.

REFERENCES

Cornwell, L. R. and Schapery, R. A. (1975) SEM study of microcracking in strained solid propellant. *Metallography* **8,** 445–452.

Farris, R. J. (1968) The character of the stress-strain function for highly filled elastomers. *Tran. Soc. Rheology* **12,** 303–314.

Farris, R. J. (1983) Mechanical behavior and dilatation of particulate-filled thermosets in the rubbery state. *J. Appl. Polymer Sci.* **28,** 3369–3386.

Ferry, J. D. (1980) *Viscoelastic Properties of Polymers*, 3rd edn. Wiley, New York.

Gent, A. N. and Lindley, P. B. (1958) Internal rupture of bonded rubber cylinders in tension. *Proc. Royal Society A* Vol. 249, pp. 195–205.

Hufferd, W. L. (1980) Thermal-mechanical interaction in filled polymers. In *Proc. of the NSF Workshop on a Continuum Mechanics Approach to Damage and Life Prediction*, Carrollton, KY.

Lamborn, M. J. and Schapery, R. A. (1988) An investigation of deformation path-independence of mechanical work in fiber-reinforced plastics. In *Proc. 4th Japan-U.S. Conference of Composite Materials*, ASME Special Technical Publication, Book No. AMD-Vol. 92, pp. 991–1000.

Lamborn, M. J. and Schapery, R. A. (1993) An investigation of the existence of a work potential for fiber-reinforced plastic. *J. Comp. Mat.* **27,** 352–382.

Mullins, L. (1969) Softening of rubber by deformation. *Rubber Chem. Tech.* **42,** 339–362.

Park, S. W. (1994) Development of a nonlinear thermo-viscoelastic constitutive equation for particulate composites with growing damage. Ph.D. dissertation, The University of Texas, Austin, Texas.

Peng, S. T. J. (1985) Nonlinear multiaxial finite deformation investigation of solid propellant. *Air Force Propulsion Laboratory Report AFRPL-TR-84-036.*

Peng, S. T. J. (1992) Constitutive equations of solid propellant with volume dilatation under multiaxial loading—theory of dilatation and dewetting criterion. *JANNAF Propulsion Meeting*, 24–27 February, Indianapolis, Indiana.

Schapery, R. A. (1974) A nonlinear constitutive theory for particulate composites based on viscoelastic fracture mechanics. In *Proc. of the 11th Meeting of the JANNAF Structures & Mechanical Behavior Working Group*, Chemical Propulsion Information Agency, Publication No. 253.

Schapery, R. A. (1975) A theory of crack initiation and growth in viscoelastic media. Part III: analysis of continuous growth. *Int. J. Fracture* **11,** 549–562.

Schapery, R. A. (1981) On viscoelastic deformation and failure behavior of composite materials with distributed flaws. In 1981 *Advances in Aerospace Structures and Materials* (S. S. Wang and W. J. Renton), ASME, New York, AD-01, pp. 5–20.

Schapery, R. A. (1982) Models for damage growth and fracture in nonlinear viscoelastic particulate composites. In *Proc. Ninth U.S. National Congress of Applied Mechanics*, Book No. H00228 (ed. Y. H. Pao), ASME, New York, pp. 237–245.

Schapery, R. A. (1984) Correspondence principles and a generalized J integral for large deformation and fracture analysis of viscoelastic media. *Int. J. Fracture* **25,** 195–223.

Schapery, R. A. (1987a) Deformation and fracture characterization of inelastic composite materials using potentials. *Polymer Engng and Sci.* **27,** 63–76.

Schapery, R. A. (1987b) Nonlinear constitutive equations for solid propellant based on a work potential and micromechanical model. In *Proc.* 1987 *JANNAF Structures and Mechanical Behavior Meeting*, 17–19 March, CPIA, Huntsville, AL.

Schapery, R. A. (1989) Mechanical characterization and analysis of inelastic composite laminates with growing damage. *Mech. Comp. Mat. and Structures*, ASME AMD, **100,** 1–9.

Schapery, R. A. (1990a) A theory of mechanical behavior of elastic media with growing damage and other changes in structure. *J. Mech. Phys. Solids* **38,** 215–253.

Schapery, R. A. (1990b) Simplifications in the behavior of viscoelastic composites with growing damage. In *Proc. IUTAM Symposium in Inelastic Deformation of Composite Materials*, Troy, New York, (ed. G. J. Dvorak), Springer, New York-Wien, pp. 193–214.

Schapery, R. A. (1991) Analysis of damage growth in particulate composites using a work potential. *Comp. Engng* **1,** 167–182.

Schapery, R. A. and Sicking, D. L. (1995) On nonlinear constitutive equations for elastic and viscoelastic composites with growing damage. In *Mechanical Behavior of Materials* (ed. A. Bakker), Delft University Press, Delft, The Netherlands, pp. 45–76.

Simo, J. C. (1987) On a fully three-dimensional finite strain viscoelastic damage model: formulation and computational aspects. *Computer Methods in Appl. Mech. Engng* **60,** 153–173.

Swanson, S. R. and Christensen, L. W. (1983) A constitutive formulation for high-elongation propellants. *J. Spacecraft Rockets* **20,** 559–566.